ORIGINAL RESEARCH

American Society of Plant Biologists   S·E·B SOCIETY FOR EXPERIMENTAL BIOLOGY   WILEY

Utilizing random regression models for genomic prediction of a longitudinal trait derived from high-throughput phenotyping

Malachy Campbell[1] | Harkamal Walia[1] | Gota Morota[2]

[1]Department of Agronomy and Horticulture, University of Nebraska Lincoln, Lincoln, Nebraska

[2]Department of Animal and Poultry Sciences, Virginia Polytechnic Institute and State University, Blacksburg, Virginia

Correspondence
Malachy Campbell, Department of Agronomy and Horticulture, University of Nebraska Lincoln, Lincoln, NE 68583.
Email: campbell.malachy@gmail.com

Abstract

The accessibility of high-throughput phenotyping platforms in both the greenhouse and field, as well as the relatively low cost of unmanned aerial vehicles, has provided researchers with an effective means to characterize large populations throughout the growing season. These longitudinal phenotypes can provide important insight into plant development and responses to the environment. Despite the growing use of these new phenotyping approaches in plant breeding, the use of genomic prediction models for longitudinal phenotypes is limited in major crop species. The objective of this study was to demonstrate the utility of random regression (RR) models using Legendre polynomials for genomic prediction of shoot growth trajectories in rice (*Oryza sativa*). An estimate of shoot biomass, projected shoot area (PSA), was recorded over a period of 20 days for a panel of 357 diverse rice accessions using an image-based greenhouse phenotyping platform. A RR that included a fixed second-order Legendre polynomial, a random second-order Legendre polynomial for the additive genetic effect, a first-order Legendre polynomial for the environmental effect, and heterogeneous residual variances was used to model PSA trajectories. The utility of the RR model over a single time point (TP) approach, where PSA is fit at each time point independently, is shown through four prediction scenarios. In the first scenario, the RR and TP approaches were used to predict PSA for a set of lines lacking phenotypic data. The RR approach showed a 11.6% increase in prediction accuracy over the TP approach. Much of this improvement could be attributed to the greater additive genetic variance captured by the RR approach. The remaining scenarios focused forecasting future phenotypes using a subset of early time points for known lines with phenotypic data, as well new lines lacking phenotypic data. In all cases, PSA could be predicted with high accuracy (r: 0.79 to 0.89 and 0.55 to 0.58 for known and unknown lines, respectively). This study provides the first application of RR models for genomic prediction of a longitudinal trait in rice and demonstrates that RR models can be effectively used to improve the accuracy of genomic prediction for complex traits compared to a TP approach.

KEYWORDS
genetics, genomic prediction, high-throughput phenotyping, phenomics

1 | INTRODUCTION

With the advent of next-generation sequencing technologies, the biology community has experienced a rapid increase in the amount of genotypic data that is available. These developments, along with the low cost of sequencing, have encouraged the adoption of genomic selection (GS) approaches in plant breeding. With these approaches, genome-wide SNP markers are used to estimate an individuals additive genetic contribution to a given trait, and genotyped individuals can be selected and advanced to further generations without phenotypic evaluation (Endelman, 2011; Jannink, Lorenz, & Iwata, 2010; Meuwissen, Hayes, & Goddard, 2001). Although these approaches have increased genetic gain through the acceleration of breeding cycles, considerable resources must still be devoted to the accurate phenotypic evaluation of individuals (Furbank & Tester, 2011). This necessary step remains a major bottleneck for many breeding programs.

In recent years, considerable investment, in both the public and private sector, has been made to automate the phenotypic characterization of large populations. Large investments have been made to build high-throughput phenotyping facilities in both the greenhouse and field where highly controlled water, nutrient, or temperature regimes can be applied to individual plots, and plants can be routinely monitored throughout the development using imaging. Moreover, the relatively low cost of drones that can be fitted with cameras and other sensors has provided researchers with an effective means to characterize large populations throughout the growing season (Chapman et al., 2014; Furbank & Tester, 2011; Watanabe et al., 2017; Zhang et al., 2016). These longitudinal phenotypes can provide important insight into the mechanisms that underlie physiological responses to environmental stresses and developmental processes, and can be leveraged to improve prediction accuracies for complex polygenic traits, such as yield that have been a target for most breeding programs (Campbell et al., 2017; Fahlgren, Gehan, & Baxter, 2015; Sun et al., 2017). Despite the growing use of these new phenotyping approaches in plant breeding, the use of models for genomic selection (GS) for longitudinal phenotypes is limited in breeding major crop species. Most conventional field studies involve one or a few evaluations throughout the growing season, thus repeated phenotypic measurements on the same plant or plot are relatively rare.

Several approaches have been utilized for GS using longitudinal data. A simple repeatability (SR) model was used by Sun et al. (2017) and Rutkoski et al. (2016) for secondary longitudinal traits. The SR model treats each time point as a repeated measure of the same trait and assumes that the variance for all records is equal and the correlation between time points is constant. However, for many traits recorded across many time points, the assumption behind SR model is not realistic. A multivariate approach can be extended to longitudinal data. However, the computational complexity of the multivariate approach increases with the number of time points and becomes unfeasible with high frequency longitudinal traits due to the large number of parameters to estimate. Often, the number of observations necessary to accurately estimate parameters exceeds the size of most studies.

Random regression (RR) models have proven to be an attractive alternative to the above methods and have been utilized in livestock and tree breeding (Apiolaza, Gilmour, & Garrick, 2000; Bermejo et al., 2003; Bohmanova, Miglior, Jamrozik, Misztal, & Sullivan, 2008; Costa et al., 2008; Howard et al., 2015; Nobre et al., 2003; Wetten, Ødegård, Vangen, & Meuwissen, 2012). Here, covariance functions are explicitly defined that are equivalent to the full covariance matrix of the trait across time points (Kirkpatrick, Lofsvold, & Bulmer, 1990; Meyer, 1998). Covariance functions include, but are not limited to banded correlation, autoregressive models, orthogonal polynomials, or spline functions (Apiolaza et al., 2000; Meyer, 1998). Thus, these models utilize a few parameters to describe the full covariance and are much more computationally efficient. In animal breeding, RR models have been used extensively to estimate heritabilities and perform pedigree-based prediction of important longitudinal traits such as growth, feed intake, fat, and milk production (Bermejo et al., 2003; Bohmanova et al., 2008; Costa et al., 2008; Howard et al., 2015; Nobre et al., 2003; Wetten et al., 2012).

The increased accessibility to high-throughput phenotyping platforms provides the plant science community with high frequency temporal measurements for complex polygenic phenotypes. These data are very different from those typically used for genomic prediction in which phenotypes are recorded at a single time point or at harvest for large populations. However, the availability of these new data presents an opportunity to extend these approaches used extensively for longitudinal traits in animal breeding to major crops. Here, we demonstrate the use of RR models to predict shoot growth trajectories in a rice diversity panel. Specifically, the aims of this study were to (a) examine the advantage of utilizing longitudinal phenotypes over single end-point measurements (cross-sectional GS), (b) determine whether longitudinal phenotypes collected during early time points can be used to predict phenotypes at later time points (i.e., forecasting lines with records), and (c) predict future phenotypes for new lines using early records for existing lines.

2 | MATERIALS AND METHODS

2.1 | Plant materials and greenhouse conditions

Three hundred seventy-eight lines of the Rice Diversity Panel 1 were selected for this study (Zhao et al., 2011). Seed propagation is described in Campbell et al. (2015). Three uniformly germinated seedlings were selected and transplanted to pots (150 mm diameter × 200 mm height) filled with approximately 2.5 kg of UC Mix (the actual weight varied from experiment to experiment by 100–200 g). Square containers were placed below each pot to allow water to collect.

2.2 | Experimental design

All experiments were conducted at the Plant Accelerator, Australian Plant Phenomics Facility, at the University of Adelaide, SA, Australia.

Each experiment consisted of 378 lines and was repeated three times from February to April 2016. Two smarthouses were used for each experiment, with 216 pots positioned across 24 lanes in each smarthouse. Each experiment consisted of a partially replicated design, with 54 randomly selected lines having two replicates in each experiment.

Seven days after transplant (DAT), plants were thinned to one seedling per pot. Two layers of blue mesh were placed on top of the pots to reduce soil water evaporation. The plants were loaded on the imaging system and were watered to 90% field capacity at 11 DAT.

2.3 | Image analysis

The plants were imaged daily from 13 to 33 DAT using a visible (red–green–blue camera; Basler Pilot piA2400–12 gc, Ahrensburg, Germany) from two side-view angles separated by 90° and a single top view. The three experiments produced a total of 72,537 images. "Plant pixels" were extracted from RGB images using the LemnaGrid software. In brief, "plant pixels" were extracted from background objects using a color classification strategy. Two set of colors were chosen manually to represent plant and background objects. For each image, pixels were assigned as background or plant pixels using the nearest-neighbor method. For a given pixel, this method assigns the pixel to a predefined color by finding the most similar (smallest Euclidean distance) color in the set. Noise (i.e., small areas of non-plant pixels) in the image is removed using a series of erosion and dilation steps.

The sum of the "plant pixels" from the three RGB images was summed, and used as a measure of shoot biomass. Here this trait is referred to as projected shoot area (PSA). This metric has been shown to be an accurate representation of shoot biomass (Campbell et al., 2015; Golzarian et al., 2011; Knecht, Campbell, Caprez, Swanson, & Walia, 2016). Prior to downstream analyses, outlier plants at each time point were detected for each trait using the 1.5(IQR) rule. Plants that were flagged as potential outliers were plotted and inspected visually. Those that exhibited abnormal growth patterns were removed. A total of 32 plants were removed, leaving a total of 2,604 plants for downstream analyses.

2.4 | Selection of random regression models

PSA was modeled across all 20 time points using several RR models. Following the notation of Mrode (2014), the RR models can be summarized as

$$\text{PSA}_{tjk} = \mu + \sum_{k=0}^{2}\phi(t)_{jk}\beta_k + \sum_{k=0}^{nr}\phi(t)_{jk}u_{jk} + \sum_{k=0}^{nr}\phi(t)_{jk}s_{jk} + e_{tjk}$$

here β is the fixed second-order Legendre polynomial to model the overall trend in the trait overtime, u_{jk} and s_{jk} are the kth random regression coefficients for additive genetic effect and random experiment of line j, nr is the order of polynomial for the random effects, and e_{tjk} is the random residual. The order of β was selected based on visual inspection of the trends. Various polynomial functions and

residual variance structures were evaluated for line and experiment, and residuals, respectively. A complete description of the models is provided in Supporting Information Table S1. For each trait, the models were ranked based on goodness-of-prediction using Akaike's information criterion (AIC) scores (Akaike, 1974).

2.5 | Genomic selection at each time point

A mixed model approach was used to fit genomic best linear unbiased predictions (gBLUPs) at each time point using the following model.

$$\mathbf{y} = \mathbf{Zu} + \mathbf{Qs} + \mathbf{e},$$

here, $\mathbf{y}$ is the PSA at time t; $\mathbf{Z}$ and $\mathbf{Q}$ are incidence matrices corresponding to the random additive genetic effect ($\mathbf{u}$), and random experimental effect ($\mathbf{s}$), respectively; and $\mathbf{e}$ is the random residual error. For the random terms, we assume $\mathbf{u} \sim N(0, \mathbf{G}\sigma_g^2)$, $\mathbf{s} \sim N(0, \mathbf{I}\sigma_s^2)$, and $\mathbf{e} \sim N(0, \mathbf{I}\sigma_e^2)$. Here, σ_g^2 is the additive genetic variance; σ_s^2 is an environmental variance associated with experiment; and σ_e^2 is the residual variance. A genomic relationship matrix ($\mathbf{G}$) was calculated following VanRaden (2008).

$$\mathbf{G} = \frac{\mathbf{Z_{cs}Z'_{cs}}}{m}$$

here, $\mathbf{Z_{cs}}$ is a centered and scaled $n \times m$ matrix, where m is 33,674 SNPs and n is the 357 genotyped rice lines.

2.6 | Genomic selection using random regression

For each trait, the "best" random regression model was used to predict gBLUPs. The following mixed model was used to predict gBLUPs

$$\text{PSA}_{tjk} = \mu + \sum_{k=0}^{2}\phi(t)_{jk}\beta_k + \sum_{k=0}^{2}\phi(t)_{jk}u_{jk} + \sum_{k=0}^{1}\phi(t)_{jk}s_{jk} + e_{tjk}$$

The variables are the same as in Section 2.4, however, note that nr has been replaced with 2 and 1 for the additive genetic and experiment effect, respectively. Thus the random additive genetic effects are described using a second-order Legendre polynomial, while a first-order Legendre polynomial is used to describe the experiment effects across time points.

In matrix notation, the model is

$$\mathbf{y} = \mathbf{Zu} + \mathbf{Qs} + \mathbf{e},$$

with all vectors and matrices defined as above. However here u is now a vector of random regression coefficients for the additive genetic effects. For the random terms, we assume $\mathbf{u} \sim N(0, \mathbf{G} \otimes \mathbf{\Omega})$, $\mathbf{s} \sim N(0, \mathbf{I} \otimes \mathbf{P})$, and $\mathbf{e} \sim N(0, \mathbf{I} \otimes \mathbf{D})$. Here, $\mathbf{\Omega}$ is a 3×3 covariance matrix of random regression coefficients for additive genetic effects; $\mathbf{P}$ is a 2×2 covariance matrix of random regression coefficients for experiment effect; and $\mathbf{D}$ is a diagonal matrix allowing for heterogeneous variances over time points. $\mathbf{Z}$ and $\mathbf{Q}$ are covariable matrices where the ith row contains the orthogonal polynomials for the ith day of imaging. Thus, matrix $\mathbf{Z}$ is the covariable matrix for the additive genetic effects with a dimension of $t \times nk$ where nk is the order

of Legendre polynomial for the additive genetic effect multiplied by the number of individuals with phenotypic records and t refers to the number of days of imaging. Similar to that, $\mathbf{Z}$ is a $t \times ns$ covariable matrix for the experiment effect, where ns is the the order of the Legendre polynomial for the experiment effect (e.g., 1) time the number of experiments (e.g., 3). Variance components and gBLUPs were obtained using ASREML (Release 4.0) (Gilmour, Gogel, Cullis, Welham, & Thompson, 2015).

Using the method above, variance components were obtained for additive genetic and environmental components. For the additive genetic term, each line has three random regression coefficients ($nr = 0,1,2$). gBLUPs were predicted at each time point according to Mrode (2014). For a given line, j, at time t the gBLUPs can be obtained by $gBLUP_{jt} = \phi_t \hat{u}_j$; where ϕ_t is the row vector of the matrix of Legendre polynomials of order 2.

2.7 | Estimation of narrow sense heritability

To estimate the narrow sense heritability, variance components were obtained for each random term using ASREML for the TP analyses and the RR approach. For the RR approach, additive genetic variance was obtained at each time points using methods described by Mrode (2014). In brief, for time i the genetic variance can be obtained by $\mathbf{t}_i \Omega \mathbf{t}'_i$, where $\mathbf{t}_i = \phi_{ik}$, the ith row vector of the matrix of Legendre polynomials at different time points (φ) for the ith day of imaging, Ω is the covariance matrix of RR coefficients for the genetic effects, and k is the order of fit. The variance of the experimental effect across time points was calculated using the same approach. For both the single time point analysis h^2 was estimated as $\sigma_g^2/(\sigma_g^2 + \sigma_s^2 + \sigma_e^2)$.

2.8 | GS scenarios and cross-validation

Four scenarios were tested using GS (Figure 1). In the first scenario (scenario A), all 20 time points were used to fit a RR model and phenotypes were predicted for a set of lines without phenotypic records. The second scenario (scenario B), the dataset was split into two datasets each consisting of 10 consecutive time points. A RR model was fitted using the first 10 time points and was used to predict the phenotypes for the same set of lines in the last 10 time points. Scenario C can be thought of as a combination of scenarios A and B. Here, the dataset was split into four subsets, with each quadrant consisting of 178 to 179 lines and 10 time points. Here, a RR model was fitted using 10 early time points for half the lines with known phenotypes and was used to predict the phenotypes in the last 10 time points for the remaining 178 to 179 lines. At last, in the last scenario (Scenario D) we sought to predict the shoot biomass at a later time points in an independent study. This can be thought of as forecasting for new lines in an independent study. A publicly available dataset was used in which 359 lines (357 lines in common between the two studies) were phenotyped from 20 to 40 days after transplant, thus a 13 day overlap was available for the two datasets, and a RR model was fitted using phenotypic information from the time points in the first experiment for 179 lines, and was

used to predict gBLUPs for the remaining 178 lines in a second independent experiment described by (Campbell et al., 2017).

To assess the accuracy of gBLUPs for the TP GS as well as scenarios A, C, and D, a two-fold cross-validation approach was used. In brief, the 357 lines were split into two sets, with one serving as a training set with known phenotypes and the second serving as a testing set with unknown phenotypes. Since the number of lines was not even the remaining line was assigned to the training set. The accuracy of prediction was assessed by comparing predicted gBLUPs with observed PSA at each of the three experiments using Pearson's correlation method. The lines were randomly assigned to each fold, and the process was repeated 20 times. For each fold, the average correlation over the three experiments was used, and the average over the two folds was used for each resampling run. For scenario B, half of the lines were randomly selected and the first 10 time points were used to predict the phenotypes in the last 10 time points for the same lines. Again, the variance in prediction accuracy was assessed by randomly sampling half the lines for analysis. Pearson's correlation was computed for the gBLUPs and PSA as described above.

3 | RESULTS

A rice diversity panel was phenotyped over a period of 20 days during the early vegetative stage using an automated high-throughput phenotyping platform. The panel consists of 357 lines from 80 countries and captures much of the genetic diversity within cultivated rice (Zhao et al., 2011).

The plants were imaged each day using RGB cameras from three angles (two side-view angles separated by 90° and one top view). The plant pixels from each image were summed and used to estimate shoot biomass. Here, this metric is referred to as PSA and has been shown to be an accurate measure of shoot biomass in cereals (Berger, Parent, & Tester, 2010; Campbell et al., 2015). This experiment captures the early vegetative stage of development, where shoot biomass increases nearly exponentially (Figure 2a, Supporting Information Figure S1).

3.1 | Random regression model selection

RR models have been used extensively to model longitudinal phenotypes in animal breeding. These models are particularly advantageous in that differences in the shape of the curve can be accounted for, and can be solved using the conventional mixed model framework. Thus, in the scope of genetics, these models allow for inter-individual variation in the mean trend to be estimated. Here, the overall mean growth trend was modeled using a second-order Legendre polynomial. A total of eight models were evaluated to identify a model that adequately described the data and could be used for GS. Each model included a fixed second-order Legendre polynomial to describe the overall mean growth trend, while several Legendre polynomials ranging from zero to second-order Legendre polynomials
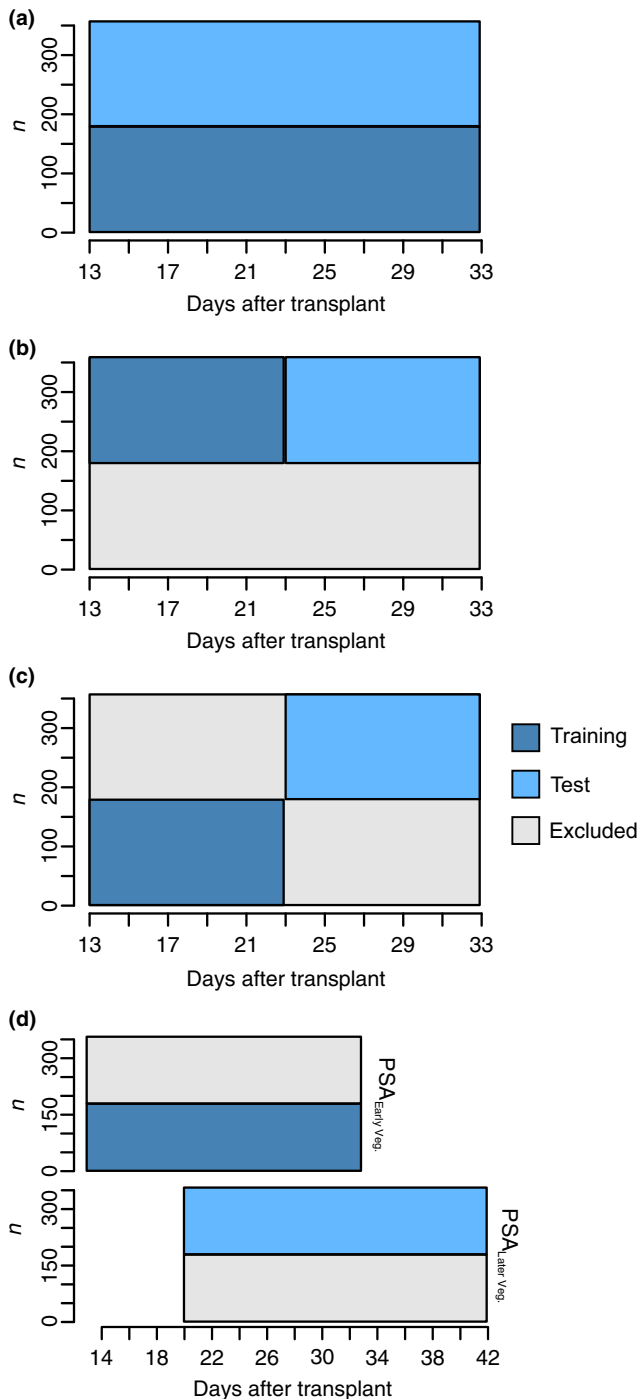
FIGURE 1 Graphic representation of cross-validation schemes for predicting longitudinal phenotypes using random regression. In (a), (c), and (d), two-fold cross-validation was used, where phenotypes for 179 lines were used as a training set to predict phenotypes for the remaining 178 lines. In (a), all 20 time points for the training set were used to predict the phenotypes at each of the 20 time points for an new set of lines. The second scenario (b) can be thought of as a forecasting approach where the dataset was split into two longitudinal datasets each consisting of 10 time points. The first 10 time points for 179 lines and were used to predict the phenotypes at the last 10 time points for the same 179 lines. In (c), a forecasting approach was again used, however, the lines were randomly split in two, and the first 10 time points were used to predict phenotypes in the last 10 time points for a group of new lines. In (d), the first 20 time points were used to predict gBLUPs at a later time points in an independent study. Here, a publicly available dataset was used as a testing set in which 357 lines were phenotyped from 20 to 40 days after transplant, thus a 13-day overlap was available for the two datasets. Here, the independent dataset is indicated with $PSA_{LaterVeg}$. Excluded indicates that these data points were not included for analyses
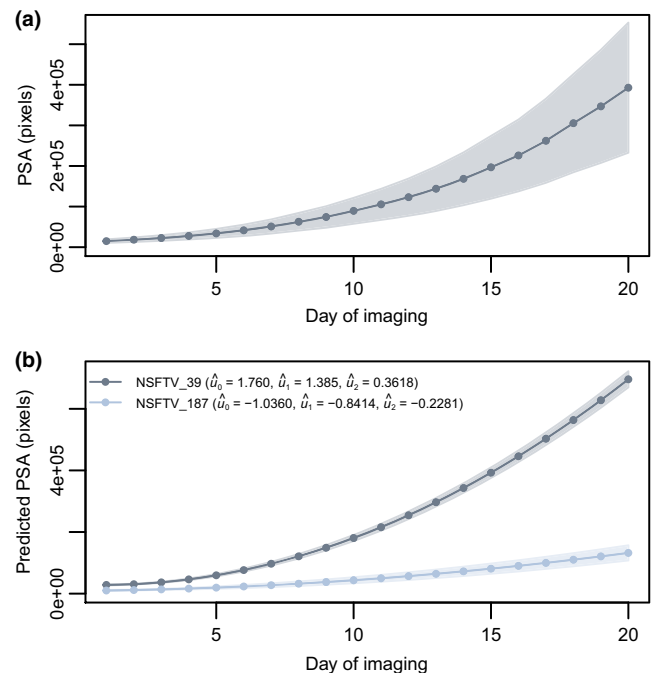
FIGURE 2 Projected shoot area (PSA) across 20 days of imaging. (a) Population mean for PSA across the 20 days of imaging. Here, the shaded region represents the standard deviation of PSA at each time point. (b) Predicted PSA for two contrasting lines using a random regression (RR) model. The RR model included a fixed second-order polynomial to model the mean trend in shoot growth, a second-order Legendre polynomial for the random additive genetic effect, a first-order Legendre polynomial for the experimental effect, and the residual variance was assumed to be heterogeneous over time points. The predicted RR coefficients for each line are provided in the figure legend. The shaded regions represent the standard error of predicted PSA at each time point. Here, PSA is defined as the sum of plant pixel from three images (two side-view images and one top view). The shaded region represents the standard deviation of PSA at each time point

were fitted for random genetic and experimental effects. The residual effects were assumed to be constant or heterogeneous across time points using an identity or diagonal matrix, respectively. The "best" model was selected based on the smallest AIC value. Supporting Information Table S1 provides an overall summary of the models and the corresponding AIC values. The "best" model (Model 8) was one that included a fixed second-order polynomial to model the mean trend in shoot growth, a second-order Legendre polynomial for the random additive genetic effect, a first-order Legendre polynomial for the experimental effect, and the residual variance was

assumed to be heterogeneous over time points. Figure 2b shows the predicted PSA obtained with model 8 for two lines with contrasting genetic values for the RR coefficients.

3.2 | Genetic correlation and narrow sense heritability of PSA

To examine the relationship for PSA between time points, the phenotypic and genetic correlation was estimated. Estimates for the overall phenotypic correlations were high (r: 0.49–1.0), with the highest correlation observed between adjacent time points (Figure 3a). The genetic correlation followed a similar patten, with an overall high correlation (r: 0.84–1.0) observed among pairwise comparisons of all 20 time points. As above, adjacent time points exhibited the highest genetic correlation ($r = 1$), while those further apart exhibited lower correlation (Figure 3b). In an interesting manner, a strong genetic correlation was observed between day 1 and day 20 ($r = 0.91$), indicating that shoot growth (e.g., PSA) may be driven by similar genetic mechanisms at the early seedling and active tillering stage in rice.

To evaluate the ability of the longitudinal RR approach to capture additive genetic variance, the narrow sense heritability of PSA was estimated using the RR model described above and a conventional mixed model at each time point. The mixed model included random terms for the additive genetic and experimental effect. For both models, a genomic relationship matrix was generated using

33,674 markers for the 357 lines. On average, the RR approach showed a 44% increase in the heritability of PSA compared to the TP approach (Figure 4). The TP approach showed a mean h^2 of 0.50 over all time points, while the RR approach showed h^2 of 0.71 on average. h^2 ranged from 0.60 to 0.77 for the RR approach, while h^2 ranged from 0.46 to 0.57 for the TP approach. The two approaches showed nearly identical h^2 estimates on day 1, however, at later time points h^2 of RR was considerably higher than TP. These results suggest that the RR approach captures more additive genetic variance for PSA than the TP approach.

3.3 | Utility of longitudinal phenotypes for genomic prediction

The availability of high-throughput phenotyping platforms provides a means to accurately phenotype large populations for a number of traits throughout time. While phenotypes recorded at a high frequency over time will likely improve the accuracy of GS, few reports have demonstrated the advantages of longitudinal phenotypes in major crops or model plant systems. Here, the utility of longitudinal phenotypes for GS was evaluated under four hypothetical scenarios (Figure 1). The first scenario can be thought of as a standard GS approach (Figure 1a). Here, all 20 time points for half of the 357 lines used to predict the phenotypes at all 20 time points for the remaining lines. The aim of scenario A is to determine whether the longitudinal
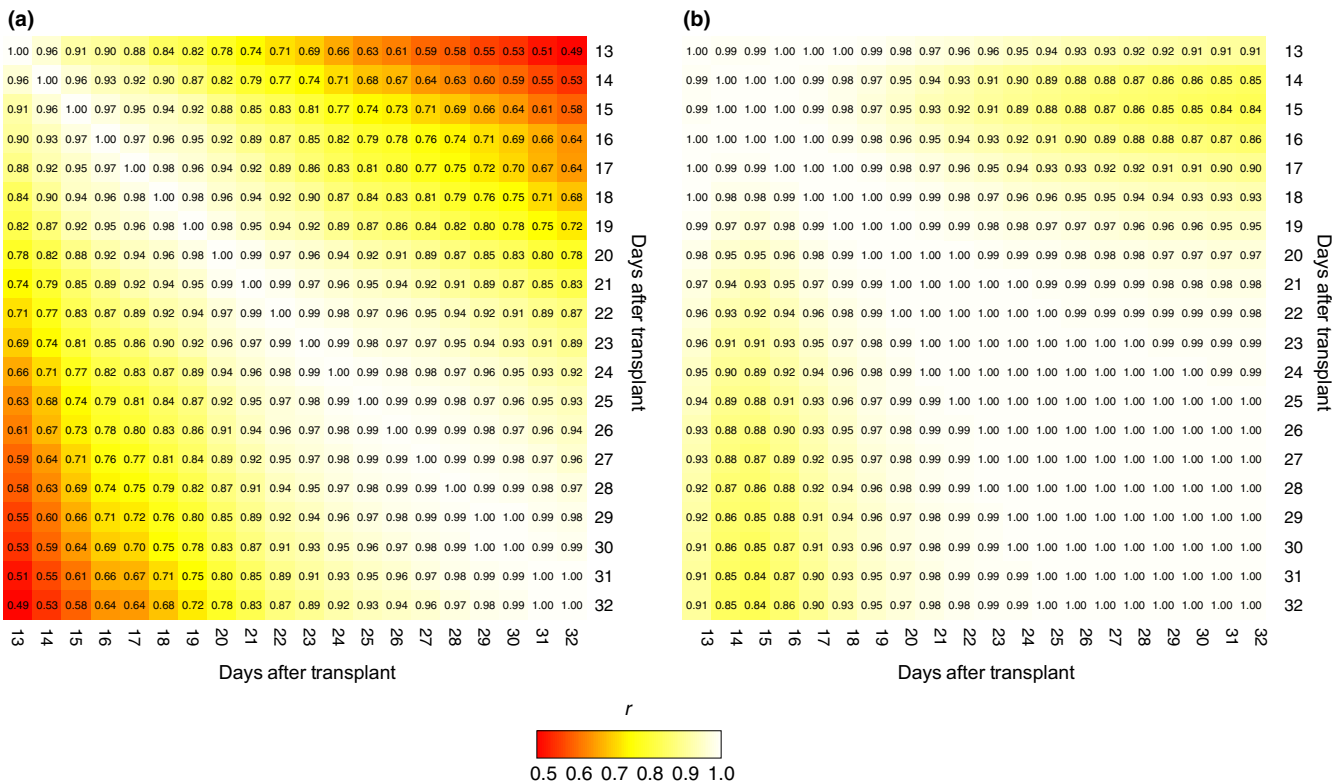
FIGURE 3 Phenotypic and genetic correlations between each time point. (a) Phenotypic correlations were estimated between time points using Pearson's method. (b) The inferred genetic correlation matrix of random regression terms for the additive genetic effects was used to estimate the genetic correlations between time points. The scale on the left of each panel indicates the strength of the correlations (r)
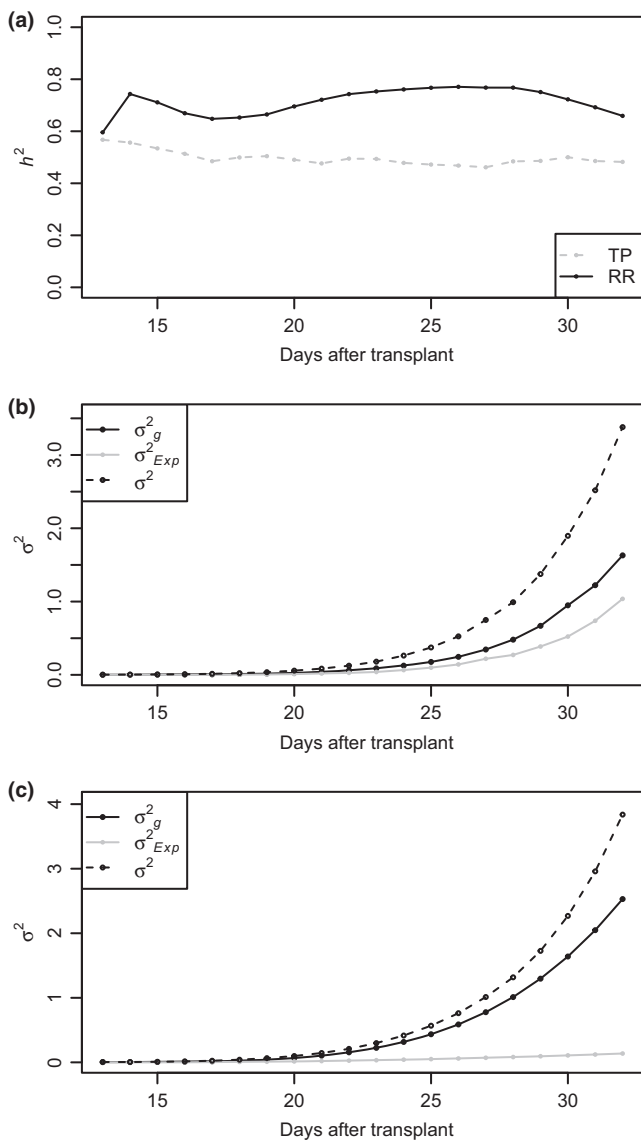
FIGURE 4 Narrow sense heritability and variance components estimated using the single time point (TP) and random regression (RR) approaches. The narrow sense heritability (h^2) is presented in panel a. Variance components for the TP and RR approaches are pictured in panels b and c, respectively. For the single time point analysis, a conventional mixed model was used to estimate the narrow sense heritability of PSA at each time point. The TP model included a random additive genetic effect and experimental effect. The RR model included a fixed second-order Legendre polynomial, the random additive genetic effect was modeled using a second-order Legendre polynomial, a first-order random effect was used for experiment, and the residual variance was assumed to be heterogeneous over time points. For both models, the experimental term was considered as an environmental effect

RR approach provides greater prediction accuracy than a cross-sectional GS approach in which a mixed model is fit at each time point. The first training set can be thought of as existing lines with phenotypic records and the test population as a new set of lines without records. The aim of scenario B (Figure 1b), is to determine if traits at

later time points can be predicted for known lines using information at early time points. Thus, it can be considered as a forecasting approach. Here, longitudinal phenotypes are available for lines during the early time points (1–10 days of imaging), and are used to predict phenotypes for the same lines at later time points. Scenario C (Figure 1c), can also be considered a forecasting approach however for new lines. Here a subset of lines with phenotypes during the first 10 time points are used to predict the phenotypes for new lines without phenotypes at the later time points. In scenario D (Figure 1d), we sought to predict the shoot biomass at a later time points in an independent study. Here, a publicly available dataset was used in which 359 lines (357 lines in common between the two studies) were phenotyped from 20 to 40 days after transplant, thus a 13-day overlap was available for the two datasets. A RR model was fitted using phenotypic information from the time points in the first experiment for 179 lines and was used to predict gBLUPs for the remaining 178 lines in the second experiment.

3.4 | Scenario A: Comparison between longitudinal RR and cross-sectional GS

To evaluate the advantages of using the longitudinal phenotype for PSA for GS over a single time points, the prediction accuracy of the RR model described above was compared to a conventional cross-sectional approach in which the additive genetic effects were estimated at each time point. For both approaches, two-fold cross-validation was performed in which half the lines were randomly selected as a training set, and the remaining half was used for prediction. Pearson's correlation was used to assess the accuracy between predicted gBLUPs and observed PSA in the test set for each experiment. The average correlation across all three experiments was determined for each fold. The resampling process was repeated 10 times.

Overall, the RR model showed significantly higher predication accuracies than the TP approach (Figure 5a). On average, the longitudinal phenotype improved prediction accuracy by 11.6% (mean across all time points) compared to the TP approach. The prediction accuracies for the TP approach ranged from 0.40 to 0.60, while for the RR approach accuracies ranged from 0.47 to 0.58. Although the TP approach exhibited low prediction accuracies during the early time points and increasing prediction accuracies toward the end of the study, the prediction accuracy for the RR model remained relatively constant with a slight increase in r observed from day 1 to 9. The largest improvements in prediction accuracy was observed between 5 to 10 days of imaging, with the RR model showing 35% higher accuracy at day 8 compared to the TP approach. Collectively, these results indicate that RR models can be used to improve the accuracy of genomic prediction for longitudinal phenotypes.

3.5 | Scenario B: Forecasting existing lines

Here, the objective is to predict future phenotypes for lines with phenotypic trajectories recorded earlier in the growing season or development. To this end, the dataset was separated into two, with
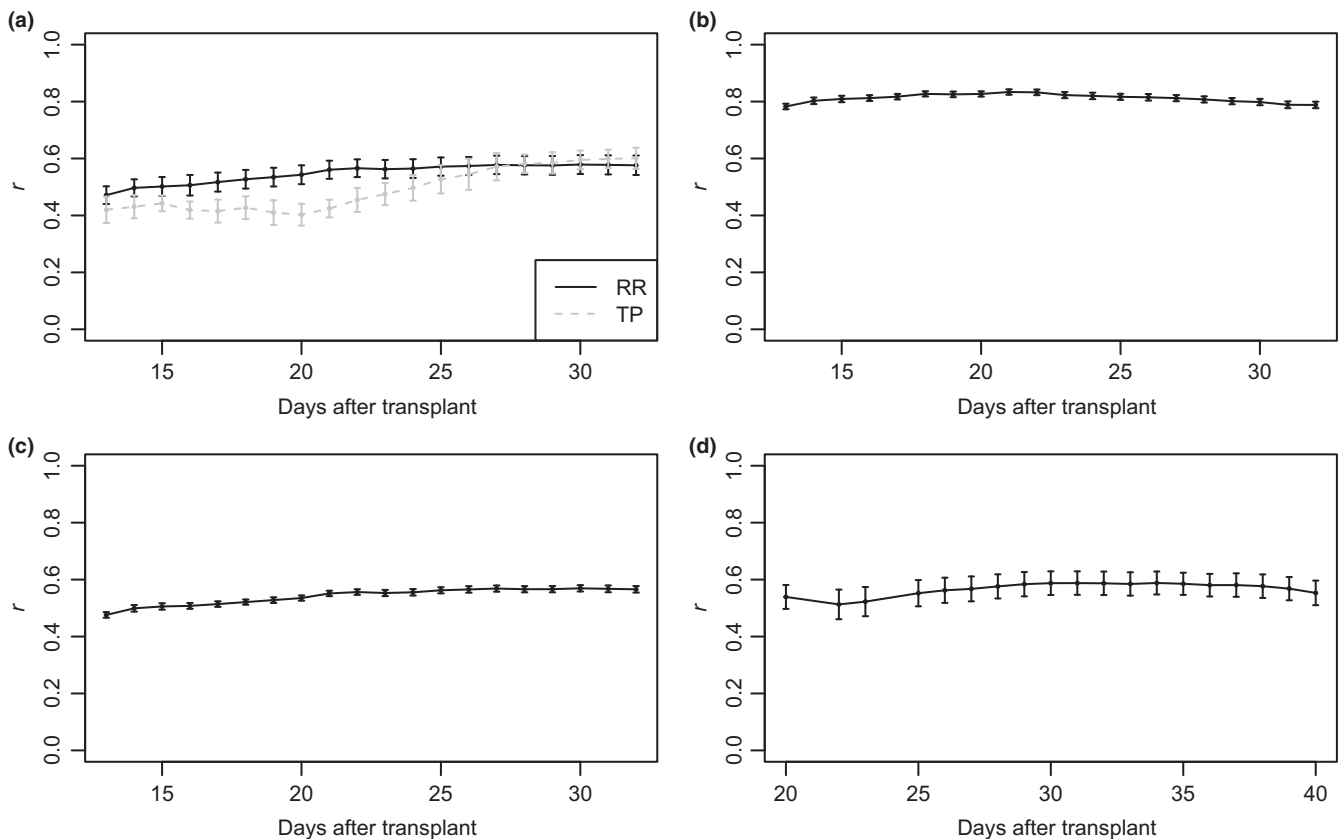
FIGURE 5 Prediction accuracies of scenarios a to d. (a) Comparison of prediction accuracies for TP and RR approaches. For the random regression (RR) approach, a RR model was fit using phenotypic records for 178–179 lines over 20 days. A univariate single time point (TP) was performed using phenotypic records for 178–179 lines at each day. In both cases, genetic effects from each model were used to predict gBLUPs for the remaining 178–179 lines, and prediction accuracy was assessed using Pearson's correlation between the predicted gBLUPs and observed PSA for the test set. Resampling was carried out 20 times. (b) Forecasting future phenotypes using phenotypic information at early time points for known lines. Here, a RR model was fit using phenotypic information for 178–179 lines for the first 10 time points, and was used to predict PSA for the same lines at the last 10 time points. Prediction accuracy was assessed using Pearson's correlation between the predicted gBLUPs and observed PSA. (c) Forecasting future phenotypes using phenotypic information at early time points for new lines. As in scenario b, a RR model was fit using phenotypic information for 178–179 lines for the first 10 time points, however the genetic effects were used to predict PSA at the last 10 time points for the remaining 178–179 lines in the test set. Prediction accuracy was assessed using Pearson's correlation between the predicted gBLUPs and observed PSA for the test set. (d) Prediction accuracies for forecasting future phenotypes in an independent study using phenotypes from an earlier developmental period. Here, a RR model was fit using phenotypic information from the first 20 time points for 178–179 lines and was used to predict PSA in an independent study at a later developmental stage for the remaining 178–179 lines. In all panels the error bars represent the standard deviation where $n = 20$

the first 10 time points serving as a training set to predict the phenotypes for the last 10 days. This approach is described in Figure 1b. The RR model described above was fit to the data. To assess the accuracy of prediction, two-fold cross-validation was performed in which 50% of the lines were randomly selected for training and prediction, and the resampling process was repeated 10 times. The accuracy of prediction was very high, ranging from 0.79 to 0.82 for the last 10 time points without phenotypic records (Figure 5b). A slight decline in prediction accuracy was observed after day 10, with day 11 exhibiting the highest accuracy ($r = 0.82$) and the lowest accuracy on day 20 ($r = 0.79$). This trend in prediction accuracy is expected, given that the phenotypic records at day 11 should be very highly correlated with those at day 10, with the correlation declining as time progresses. The high predictive ability observed indicates that the first 10 time points is sufficient to accurately predict future phenotypes for known lines.

3.6 | Scenario C: Forecasting new lines

As shown above, future phenotypes can be accurately predicted from longitudinal traits at early time points for existing lines. While the knowledge of performance of known lines at future time points may be beneficial in some applications, GS is most often used to select lines without prior knowledge of the phenotype. Previously in scenario A, we showed that phenotypes could be predicted accurately for new lines using the complete longitudinal phenotype. Here, the aim is to predict future phenotypes for new lines with no phenotypic records using early phenotypic records for existing lines. To this end, the dataset was partitioned into two temporal datasets, with the first 10 time points serving as a training set to predict the phenotypes for the last 10 days (Figure 1c). As above, a two-fold cross-validation approach was used to assess prediction accuracy. Half the lines were randomly assigned to each fold, and the first 10

CAMPBELL ET AL.

American Society
of Plant Biologists
Cultivating a better future through plant biology research

SEB
SOCIETY FOR EXPERIMENTAL BIOLOGY

WILEY | 9

time points from the first fold were used to predict the phenotypes at the last 10 time points in the second fold. The prediction accuracies for scenario C were very similar to those observed for scenario A. Accuracies ranged from 0.48 to 0.57, with the prediction accuracy ranging from 0.55 to 0.57 in the last 10 days (Figure 5c). The prediction accuracies showed a slight increase from day 1 to day 9. The highest prediction accuracy was observed at day 15, while the lowest accuracy was observed at day 1. These results suggest that future phenotypes can be forecast for new lines with reasonable accuracy using phenotypic records from earlier time points for a set of known lines.

3.7 | Scenario D: Forecasting new lines at later time points in an independent study

In scenario C, we have shown that gBLUPs for new lines can be accurately predicted using phenotypes for a set of known lines at a subset of early time points. Here, the objective was to expand this approach and evaluate the utility of the RR model to predict gBLUPs for new lines at future time points in an independent study. Here, we utilized an existing dataset where 359 lines from the Rice Diversity Panel 1 were phenotyped from 20 to 40 days after transplant (Figure 1d). Although there is overlap between developmental stages of this dataset and the dataset used for scenarios A–C, this experiment was conducted at a different time of year and therefore the photoperiod and light intensity should be different between the two.

A RR model was fitted that was identical to that used for scenarios A–C, in that it included a fixed second-order polynomial to model the mean trend in PSA, a second-order Legendre polynomial for the random additive genetic effect, a first-order Legendre polynomial for the random experimental effect, and a heterogeneous residual variance over time points. The RR model was fitted using phenotypes for 179 lines from the early vegetative stage experiment (i.e., 13 to 32 DAT), and the genetic values for the RR coefficients were used to predict the phenotypes for the remaining 178 lines in the second experiment (i.e., 20 to 40 DAT). A two-fold cross-validation approach was used in which phenotypes across all 20 days were selected for 179 lines in the first experiment and were used to predict gBLUPs for the remaining 178 lines in the second experiment.

The prediction accuracy was high with r values ranging from 0.51 to 0.59 (Figure 5d). The prediction accuracy was relatively constant, but showed a slight increase in accuracy from 22 to 29 days after transplant. An increase in the prediction accuracy was observed from 13 to 31 DAT, after which the prediction accuracy declined slightly. The second time point (22 DAT) exhibited the lowest prediction accuracy ($r = 0.51$). The highest prediction accuracy was observed on day 34 after transplant ($r = 0.59$). Collectively, these results suggest that longitudinal phenotypes can be accurately predicted in an independent study using the RR approach.

4 | DISCUSSION

High-throughput phenotyping platforms provide an accessible means to record traits non-destructively for large populations throughout development. Such longitudinal data provide an opportunity to understand the genetics of the development of a phenotype and identify individuals that exhibit desirable trait trajectories. However, such data provides new challenges to adapt approaches utilized for single time point phenotypes in plant genomics and breeding to accommodate longitudinal data. This study provides the first application of RR models for genomic prediction of a longitudinal trait in rice.

4.1 | Advantages of RR over univariate genomic prediction

The predictive ability in GS is dependent on the heritability of the trait, the number of markers, population size, linkage disequilibrium (LD), and the number of QTL influencing the trait (Daetwyler, Pong-Wong, Villanueva, & Woolliams, 2010; Daetwyler, Villanueva, & Woolliams, 2008). Here, the RR model using longitudinal phenotypes provided greater prediction accuracy compared to the TP gBLUP. The predictive ability of the RR approach improved prediction accuracies by 11.6% on average compared to TP analysis. The number of markers, population size, LD, and the number of QTL influencing PSA are held constant between the two models. Thus, the difference in prediction accuracy hold be largely attributed to the differences in heritability between the RR approach and TP analysis. As shown in Figure 4, the RR approach accounted for more additive genetic variance than the TP analysis. Similar gains in heritability for height in Swedish Scots pine has been reported by Wang, Andersson, and Waldmann (2009) with RR models that utilize B-splines or Legendre polynomials over TP analyses. Moreover, when the prediction accuracy is expressed as the ratio of the correlation of gBLUPs and observed PSA to the square root of h^2, both approaches were nearly equivalent (Supporting Information Figure S2). Thus, the higher prediction accuracy is due to the higher h^2 of the RR approach relative to the TP approach.

With both methods (RR and TP), we observed high prediction accuracies ranging from 0.4 to 0.6 (Arruda et al., 2015; Duhnen et al., 2017; Kristensen et al., 2018; Leplat, Jensen, & Madsen, 2016). While similar accuracies have been reported by other studies for complex traits, it is important to note that the current study utilized a diversity panel with considerable population stratification and the prediction models did not account for population structure. Accounting for population structure is important in genome-wide association studies to reduce spurious associations (Yu et al., 2006). However, these corrections can often hinder the ability to detect true QTL that are correlated with population structure (Zhao et al., 2011). With GS, the aim is to achieve high prediction accuracies across subpopulations rather than to detect QTL associated with the trait (Hayes, Bowman, Chamberlain, Verbyla, & Goddard, 2009; Lorenz et al., 2011). Thus, the high prediction accuracies observed for the models used in this study may be due, in part, to population structure, however, the random sampling of individuals across subpopulations during CV should reduce the possibility of having a training set that is strongly imbalanced by a given subpopulation.

4.2 | Utilizing RR prediction for forecasting phenotypes

The utilization of genomic information to predict future outcomes is not new. Considerable effort in the field of personalized medicine has been devoted to predict disease risks for individuals based on genomic information. Here, disease-associated loci are used to predict potential future outcomes for individuals (Moser et al., 2015). The ability to predict future phenotypes using phenotypic information collected early in the life cycle may be advantageous in plants, particularly perennial species with long life cycles. Selection during the early developmental stage can shorten evaluation times.

Here, we evaluated the ability of RR models to predict future phenotypes using phenotypic records collected during the early time points. This was performed for known lines (e.g., those with early records; Scenario B), as well as new lines (Scenario C and D). We observed high prediction accuracies for each forecasting scenario. As expected the highest accuracy was observed for Scenario B, in which early phenotypic records are used to predict future phenotypes for the same set of lines. In a surprising way, high prediction accuracies were also observed when early records for known lines were used to predict future phenotypes for unknown lines (Scenarios C and D). In both cases, the accuracies were not significantly different from those achieved when using phenotypic information for all time points. These results collectively indicate that the future phenotypes can be accurately predicted using a subset of the temporal phenotypes. While these results are encouraging, these forecasting approaches will be highly dependent on the temporal genetic architecture of the trait. The lack of decline by utilizing only a subset of time points is likely due to the high genetic correlation observed between time points. The similar genetic architecture between the early and late time points that is evidenced by the strong positive genetic correlation (Figure 3b) estimated between early (1–10 days) and late (11–20 days) time points. Thus, we suggest to first evaluate the genetic correlation between time points for the trait of interest before utilizing such forecasting approaches.

5 | CONCLUSION

High-throughput phenomics platforms have provided the plant science community with a means to generate high resolution temporal phenotypes for large populations at a relatively low cost. RR models that utilize Legendre polynomials provide a flexible for genomic prediction of longitudinal traits. These approaches provide several advantages over single time point analyses: (a) these models account for more additive genetic variance compared to the TP analysis, which translates to higher predictive accuracies; (b) future phenotypes can be accurately predicted using phenotypic information for earlier time points for known and unknown lines.

ACKNOWLEDGMENTS

AUTHOR CONTRIBUTIONS

Study was conceived by H.W., G.M., and M.C.; phenotyping was performed by M.C. under the supervision of H.W.; M.C. performed all analyses under the supervision of G.M.; M.C. wrote the manuscript, and editorial comments were provided by H.W. and G.M.

DATA ACCESSIBILITY

The full datasets and all code used in this study are available via GitHub (https://doi.org/10.5281/zenodo.1313684) and the WRCHR website (WRCHR.org).

REFERENCES

Akaike, H. (1974). A new look at the statistical model identification. *IEEE Transactions on Automatic Control*, *19*(6), 716–723. https://doi.org/10.1109/TAC.1974.1100705

Apiolaza, L. A., Gilmour, A. R., & Garrick, D. J. (2000). Variance modelling of longitudinal height data from a *Pinus Radiata* progeny test. *Canadian Journal of Forest Research*, *30*(4), 645–654. https://doi.org/10.1139/x99-246

Arruda, M. P., Brown, P. J., Lipka, A. E., Krill, A. M., Thurber, C., & Kolb, F. L. (2015). Genomic selection for predicting fusarium head blight resistance in a wheat breeding program. *The Plant Genome*, *8*(3), 1–12.

Berger, B., Parent, B., & Tester, M. (2010). High-throughput shoot imaging to study drought responses. *Journal of Experimental Botany*, *61*(13), 3519–3528. https://doi.org/10.1093/jxb/erq201

Bermejo, J. L., Roehe, R., Schulze, V., Rave, G., Looft, H., & Kalm, E. (2003). Random regression to model genetically the longitudinal data of daily feed intake in growing pigs. *Livestock Production Science*, *82*(2), 189–199. https://doi.org/10.1016/S0301-6226(03)00032-0

Bohmanova, J., Miglior, F., Jamrozik, J., Misztal, I., & Sullivan, P. G. (2008). Comparison of random regression models with Legendre polynomials and linear splines for production traits and somatic cell score of Canadian Holstein cows. *Journal of Dairy Science*, *91*(9), 3627–3638. https://doi.org/10.3168/jds.2007-0945

Campbell, M. T., Du, Q., Liu, K., Brien, C. J., Berger, B., Zhang, C., & Walia, H. (2017). A comprehensive image-based phenomic analysis reveals the complex genetic architecture of shoot growth dynamics in rice. *The Plant Genome*, *10*(2), 1–14.

Campbell, M. T., Knecht, A. C., Berger, B., Brien, C. J., Wang, D., & Walia, H. (2015). Integrating image-based phenomics and association analysis to dissect the genetic architecture of temporal salinity responses in rice. *Plant Physiology*, *168*(4), 1476–1489. https://doi.org/10.1104/pp.15.00450

Chapman, S. C., Merz, T., Chan, A., Jackway, P., Hrabar, S., Dreccer, M. F., … Jimenez-Berni, J. (2014). Pheno-Copter: A low-altitude, autonomous remote-sensing robotic helicopter for high-throughput field-based phenotyping. *Agronomy*, *4*(2), 279–301. https://doi.org/10.3390/agronomy4020279

Costa, C. N., Rodrigues de Melo, C. M., Packer, I. U., Ferreira de Freitas, A., Teixeira, N. M., & Cobuci, J. A. (2008). Genetic parameters for test day milk yield of first lactation Holstein cows estimated by random regression using Legendre polynomials. *Revista Brasileira de Zootecnia*, *37*(4), 602–8. https://doi.org/10.1590/S1516-35982008000400003

Daetwyler, H. D., Pong-Wong, R., Villanueva, B., & Woolliams, J. A. (2010). The impact of genetic architecture on genome-wide evaluation methods. *Genetics*, *185*(3), 1021–1031. https://doi.org/10.1534/genetics.110.116855

Daetwyler, H. D., Villanueva, B., & Woolliams, J. A. (2008). Accuracy of predicting the genetic risk of disease using a genome-wide approach.

PLoS ONE, *3*(10), e3395. https://doi.org/10.1371/journal.pone.0003395

Duhnen, A., Gras, A., Teyssèdre, S., Romestant, M., Claustres, B., Daydé, J., & Mangin, B. (2017). Genomic selection for yield and seed protein content in soybean: A study of breeding program data and assessment of prediction accuracy. *Crop Science*, *57*(3), 1325–1337. https://doi.org/10.2135/cropsci2016.06.0496

Endelman, J. B. (2011). Ridge regression and other Kernels for genomic selection with R Package rrBLUP. *The Plant Genome*, *4*(3), 250–255. https://doi.org/10.3835/plantgenome2011.08.0024

Fahlgren, N., Gehan, M. A., & Baxter, I. (2015). Lights, camera, action: High-throughput plant phenotyping is ready for a close-up. *Current Opinion in Plant Biology*, *24*, 93–99. https://doi.org/10.1016/j.pbi.2015.02.006

Furbank, R. T., & Tester, M. (2011). Phenomics–technologies to relieve the phenotyping bottleneck. *Trends in Plant Science*, *16*(12), 635–644. https://doi.org/10.1016/j.tplants.2011.09.005

Gilmour, A. R., Gogel, B. J., Cullis, B. R., Welham, S. J., & Thompson, R. (2015). *ASReml user guide release 4.1 structural specification*. Hemel Hempstead, UK: VSN International Ltd.

Golzarian, M. R., Frick, R. A., Rajendran, K., Berger, B., Roy, S., Tester, M., & Lun, D. S. (2011). Accurate inference of shoot biomass from high-throughput images of cereal plants. *Plant Methods*, *7*(1), 2. https://doi.org/10.1186/1746-4811-7-2

Hayes, B. J., Bowman, P. J., Chamberlain, A. C., Verbyla, K., & Goddard, M. E. (2009). Accuracy of genomic breeding values in multi-breed dairy cattle populations. *Genetics Selection Evolution*, *41*(1), 51. https://doi.org/10.1186/1297-9686-41-51

Howard, J. T., Jiao, S., Tiezzi, F., Huang, Y., Gray, K. A., & Maltecca, C. (2015). Genome-wide association study on Legendre random regression coefficients for the growth and feed intake trajectory on Duroc Boars. *BMC Genetics*, *16*(1), 59. https://doi.org/10.1186/s12863-015-0218-8

Jannink, J.-L., Lorenz, A. J., & Iwata, H. (2010). Genomic selection in plant breeding: From theory to practice. *Briefings in Functional Genomics*, *9*(2), 166–177. https://doi.org/10.1093/bfgp/elq001

Kirkpatrick, M., Lofsvold, D., & Bulmer, M. (1990). Analysis of the inheritance, selection and evolution of growth trajectories. *Genetics*, *124*(4), 979–993.

Knecht, A. C., Campbell, M. T., Caprez, A., Swanson, D. R., & Walia, H. (2016). Image harvest: An open-source platform for high-throughput plant image processing and analysis. *Journal of Experimental Botany*, *67*(11), 3587–3599. https://doi.org/10.1093/jxb/erw176

Kristensen, P. S., Jahoor, A., Andersen, J. R., Cericola, F., Orabi, J., Janss, L., & Jensen, J. (2018). Genome-wide association studies and comparison of models and cross-validation strategies for genomic prediction of quality traits in advanced winter wheat breeding lines. *Frontiers in Plant Science*, *9*, 69. https://doi.org/10.3389/fpls.2018.00069

Leplat, F., Jensen, J., & Madsen, P. (2016). Genomic prediction of manganese efficiency in winter barley. *The Plant Genome*, *9*(2), 1–13.

Lorenz, A. J., Chao, S., Asoro, F. G., Heffner, E. L., Hayashi, T., Iwata, H., … Jannink, J.-L. (2011). Genomic selection in plant breeding: Knowledge and prospects. *Advances in Agronomy*, *110*, 77–123. https://doi.org/10.1016/B978-0-12-385531-2.00002-5

Meuwissen, M. T., Hayes, B. J., & Goddard, M. E. (2001). Prediction of total genetic value using genome-wide dense marker maps. *Genetics*, *157*(4), 1819–29.

Meyer, K. (1998). Estimating covariance functions for longitudinal data using a random regression model. *Genetics Selection Evolution*, *30*(3), 221. https://doi.org/10.1186/1297-9686-30-3-221

Moser, G., Lee, S. H., Hayes, B. J., Goddard, M. E., Wray, N. R., & Visscher, P. M. (2015). Simultaneous discovery, estimation and prediction analysis of complex traits using a Bayesian mixture model. *PLoS Genetics*, *11*(4), e1004969. https://doi.org/10.1371/journal.pgen.1004969

Mrode, R. A. (2014). *Linear models for the prediction of animal breeding values*. Wallingford, UK: CABI. https://doi.org/10.1079/9781780643915.0000

Nobre, P. R. C., Misztal, I., Tsuruta, S., Bertrand, J. K., Silva, L. O. C., & Lopes, P. S. (2003). Analyses of growth curves of Nellore cattle by multiple-trait and random regression models. *Journal of Animal Science*, *81*(4), 918–926. https://doi.org/10.2527/2003.814918x

Rutkoski, J., Poland, J., Mondal, S., Autrique, E., González Pérez, L., Crossa, J., … Singh, R. (2016). Canopy temperature and vegetation indices from high-throughput phenotyping improve accuracy of pedigree and genomic selection for grain yield in wheat. *G3: Genes, Genomes, Genetics*, *6*(9), 2799–2808. https://doi.org/10.1534/g3.116.032888

Sun, J., Rutkoski, J. E., Poland, J. A., Crossa, J., Jannink, J.-L., & Sorrells, M. E. (2017). Multitrait, random regression, or simple repeatability model in high-throughput phenotyping data improve genomic prediction for wheat grain yield. *The Plant Genome*, *10*(2), 1–12.

VanRaden, P. M. (2008). Efficient methods to compute genomic predictions. *Journal of Dairy Science*, *91*(11), 4414–4423. https://doi.org/10.3168/jds.2007-0980

Wang, C., Andersson, B., & Waldmann, P. (2009). Genetic analysis of longitudinal height data using random regression. *Canadian Journal of Forest Research*, *39*(10), 1939–1948. https://doi.org/10.1139/X09-111

Watanabe, K., Guo, W., Arai, K., Takanashi, H., Kajiya-Kanegae, H., Kobayashi, M., … Iwata, H. (2017). High-throughput phenotyping of sorghum plant height using an unmanned aerial vehicle and its application to genomic prediction modeling. *Frontiers in Plant Science*, *8*, 1–11.

Wetten, M., Ødegård, J., Vangen, O., & Meuwissen, T. H. E. (2012). Simultaneous estimation of daily weight and feed intake curves for growing pigs by random regression. *Animal*, *6*(3), 433–439. https://doi.org/10.1017/S1751731111001832

Yu, J., Pressoir, G., Briggs, W. H., Bi, I. V., Yamasaki, M., Doebley, J. F., … Buckler, E. S. (2006). A unified mixed-model method for association mapping that accounts for multiple levels of relatedness. *Nature Genetics*, *38*(2), 203. https://doi.org/10.1038/ng1702

Zhang, J., Yang, C., Song, H., Hoffmann, W. C., Zhang, D., & Zhang, G. (2016). Evaluation of an airborne remote sensing platform consisting of two consumer-grade cameras for crop identification. *Remote Sensing*, *8*(3), 257. https://doi.org/10.3390/rs8030257

Zhao, K., Tung, C.-W., Eizenga, G. C., Wright, M. H., Liakat Ali, M., Price, A. H., … McCouch, S. R. (2011). Genome-wide association mapping reveals a rich genetic architecture of complex traits in *Oryza Sativa*. *Nature Communications*, *2*, 467. https://doi.org/10.1038/ncomms1467

SUPPORTING INFORMATION

Additional supporting information may be found online in the Supporting Information section at the end of the article.